Eur. J. Biochem. **267**, 476–486 (2000) © FEBS 2000

Thermal unfolding of G-actin monitored with the DNase I-inhibition assay
Stabilities of actin isoforms

Herwig Schüler[1], Uno Lindberg[1], Clarence E. Schutt[2] and Roger Karlsson[1]

[1]*Department of Cell Biology, The Wenner-Gren Institute, Stockholm University, Sweden;* [2]*The Henry Hoyt Laboratory, Department of Chemistry, Princeton University, New Jersey, USA*

Actin is one of the proteins that rely on chaperonins for proper folding. This paper shows that the thermal unfolding of G-actin, as studied by CD and ultraviolet difference spectrometry, coincides with a loss in DNase I-inhibiting activity of the protein. Thus, the DNase I inhibition assay should be useful for systematic studies of actin unfolding and refolding. Using this assay, we have investigated how the thermal stability of actin is affected by either Ca^{2+} or Mg^{2+} at the high affinity divalent cation binding site, by the concentration of excess nucleotide, and by the nucleotide in different states of phosphorylation (ATP, ADP.P_i, ADP.V_i, ADP.AlF_4, ADP.BeF_x, and ADP). Actin isoforms from different species were also compared, and the effect of profilin on the thermal stability of actin was studied. We conclude that the thermal unfolding of G-actin is a three-state process, in which an equilibrium exists between native actin with bound nucleotide and an intermediate free of nucleotide. Actins in the Mg-form were less stable than the Ca-forms, and the stability of the different isoforms decreased in the following order: rabbit skeletal muscle α-actin = bovine cytoplasmic γ-actin > yeast actin > cytoplasmic β-actin. The activation energies for the thermal unfolding reactions were in the range 200–290 $kJ \cdot mol^{-1}$, depending on the bound ligands. Generally, the stability of the actin depended on the degree with which the nucleotide contributed to the connectivity between the two domains of the protein.

Keywords: circular dichroism; irreversible denaturation; nucleotide binding; profilin; phosphate analogs.

Actin, the major constituent of the microfilament system of eukaryotic cells, is involved in various force generating processes. Many organisms have different actin isoforms (reviewed in [1]), whose functional significance is suggested by tissue-specific expression and differential intracellular localization. Actin consists of two major domains, each divided into two subdomains [2]. One adenine nucleotide and a divalent cation are bound with high affinity at the bottom of the central cleft between the major domains (Fig. 1). The extensive contacts between the nucleotide–cation complex and residues in all four subdomains contribute to the stability of the protein, which quickly loses its polymerizability after removal of either the nucleotide or the cation [3,4].

Monomeric actin (G-actin) binds bovine pancreatic deoxyribonuclease I (DNase I) with nanomolar affinity [5,6] and inhibits its endonuclease activity [7,8]. This has been used to develop a simple, spectrophotometric assay for the quantification of unpolymerized and filamentous actin which can be applied even to crude cell extracts [9–11]. This assay has also been used to estimate the extent of inactivation of EDTA-treated G-actin [12,13]. The DNase I-binding site on actin comprises residues in subdomains 2 and 4 (Fig. 1) [2]. Thus, DNase I-binding and enzyme-inhibiting activity of actin would be expected to be sensitive to changes in the actin interdomain relationship. Conversely, binding of DNase I to native actin would span the nucleotide-binding cleft of the molecule, clamp the two domains and hinder conformational changes in the actin.

Single-domain proteins often fold spontaneously [14–16], whereas multidomain proteins require chaperonins for their folding. Actin, with its complexity and well-established biochemistry, provides a good model for studies of folding/unfolding. Exposure of actin to denaturing conditions has revealed two stages of different sensitivity and degrees of reversibility. After an initial irreversible step during which the ability to bind nucleotide and divalent cation, polymerizability and 40% of the α-helical content is lost, a second step with total unfolding of the protein follows. The second step appears to be spontaneously reversible, whereas reversal of the initial loss of structure and biological activity requires the involvement of the chaperonin complex CCT for folding [17,18]. The details of the folding mechanism, however, remain to be determined.

This paper shows that the loss of DNase I-inhibition activity of actin at increased temperatures correlates with the thermal unfolding of actin, as seen by CD, spectropolarimetry and ultraviolet difference spectroscopy. Therefore, the spectrophotometric DNase I-inhibition assay [9] can be used as a rapid and convenient method to study the initial stages in the unfolding of actin. It offers a direct measure of the appearance of biologically active actin in experiments with folding factors such as chaperonins. Although several studies [4,19–28] have addressed the thermal stability of G-actin, systematic investigations of the effects of different ligands on the stability of isolated actin isoforms have not been conducted. Here, the

Correspondence to R. Karlsson, Department of Cell Biology, The Wenner-Gren Institute, Stockholm University, S-106 91 Stockholm, Sweden. Fax: + 46 8 159837, Tel.: + 46 8 164101, E-mail: Roger.Karlsson@cellbio.su.se

Abbreviations: T_m, melting temperature; E_a, Arrhenius activation energy; DNase I, deoxyribonuclease I.

Enzyme: deoxyribonuclease I (EC 3.1.21.1).

(Received 13 August 1999, revised 8 November 1999, accepted 16 November 1999)

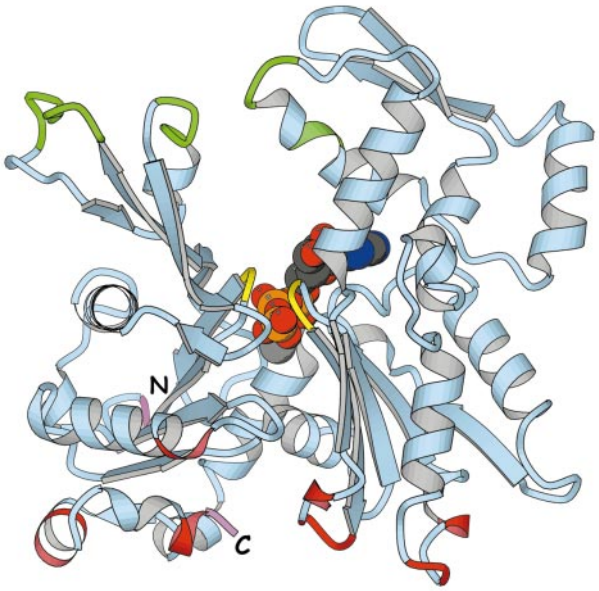

Fig. 1. Structure of β-actin with bound ATP and Sr^{2+} (PDB entry 2BTF). The residues involved in DNase I-binding in subdomains 2 and 4 [2] and profilin binding in subdomains 1 and 3 [46] are shown in green and red, respectively. The two loops binding to the ATP-phosphates are shown in yellow. The N- and C-termini are pink. Image created using MOLSCRIPT [75].

DNase I-inhibition assay is used to determine the kinetic parameters for the irreversible thermal denaturation of mammalian α, β, γ, and yeast G-actin under varying conditions. The results show that actin isoforms differ in thermal stability, and that the stability of actin depends on the nature of the bound nucleotide–cation complex and reflects differences in the linkages between the two major domains of the actin molecule mediated by these ligands. The fact that the stability was increased in direct proportion to the excess nucleotide suggests that the thermal unfolding of actin occurs *via* a nucleotide-free intermediate.

MATERIALS AND METHODS

Chemicals and protein purification

DNase I from bovine pancreas (Boehringer Mannheim GmbH, grade I) was further purified by gel filtration on Sephacryl S-200 H (Amersham Pharmacia Biotech) in 10 mM Tris/HCl pH 7.8, 0.1 M NaCl, 0.5 mM $CaCl_2$. Cytoplasmic β/γ-actin (containing 60–70% β-actin and 30–40% γ-actin) was purified from calf thymus [29]. Separation of the β and γ isoforms was achieved by hydroxyapatite chromatography [29,30] (Hypatite C, even lot number; Clarkson Chromatography Products, South Williamsport, PA, USA). Skeletal muscle α-actin was purified from rabbit muscle [31]. Yeast actin and yeast-expressed chicken β-actin were purified using DNase I-affinity chromatography and isoform separation by hydroxyapatite chromatography [6,32]. All actins were finally gel-filtered on Sephacryl S-300 (Amersham Pharmacia Biotech) or dialysed in buffer G (5 mM Tris/HCl pH 7.6, 0.1 mM $CaCl_2$, 0.5 mM ATP, 0.5 mM dithiothreitol). Actin was used within 1 week, or stored as droplets (25 μL) in liquid nitrogen. Actin concentrations were determined photometrically, using an extinction coefficient of $\varepsilon_{290\ nm} = 0.63\ mL{\cdot}mg^{-1}{\cdot}cm^{-1}$ for G-actin [33]. ADP-actin was prepared by a cycle of polymerization/depolymerization and subsequent gel filtration on S-300 in buffer G containing 0.5 mM ADP instead of ATP. Mg-actin was obtained [34] by incubation of the actins in buffer G with 0.2 mM EGTA + 50 μM $MgCl_2$. Vanadate, aluminium fluoride (AlF_4) and beryllium fluoride (BeF_x) treatment of actin was as described previously [35–37]. Profilin was purified from calf thymus as described [29]. Phalloidin (Boehringer Mannheim GmbH) was dissolved in Me_2SO to a concentration of 50 mM and further diluted in buffer G before use. The final concentration of Me_2SO never exceeded 0.1%.

DNase I-inhibition assay

The DNase I-inhibition assay was performed as described originally [9]. In brief, a DNA substrate solution (40 $\mu g{\cdot}mL^{-1}$) was prepared by dissolving salmon sperm DNA (Sigma D-1626) in 100 mM Tris/HCl pH 7.6, 4 mM $MgSO_4$, 1.8 mM $CaCl_2$. To determine the endonuclease activity of DNase I, 1 μg enzyme was mixed rapidly with 3 mL substrate solution at 25 °C, and the change in absorbance at 260 nm was recorded continuously over a period of 1–2 min using a Hewlett-Packard 8452A spectrophotometer equipped with the manufacturer's kinetics software. To determine the amount of DNase I-inhibition activity in an actin solution, 1 μg of DNase I was premixed with an amount of protein sufficient to give 30–70% inhibition of the DNase I-activity, as calculated from the ratio of the linear slopes of the absorbance increases in the absence and presence of actin.

Thermal melting curves

After establishing the DNase I-inhibition activity of monomeric actin (usually 1–10 μM) in buffer G at 25 °C, a sample was incubated at 40 °C for 10 min. Then, the sample was heated at a constant rate, and DNase I-inhibition activity was measured at 3-min intervals. The melting temperature (T_m) was taken as the temperature at which the DNase I-inhibition activity of the sample had decreased to 50% of the value determined at 25 °C. In analogy to the thermal melting of nucleic acids [38], the steepness of the transition at T_m was used as a measure of the cooperativity of the unfolding reaction. The value *a* given in Table 1 is the negative slope in T_m in a plot of the DNase I-inhibition activity (as a percentage of the value at 25 °C) vs. temperature (e.g. Fig. 2C). Thus, a higher value of *a*

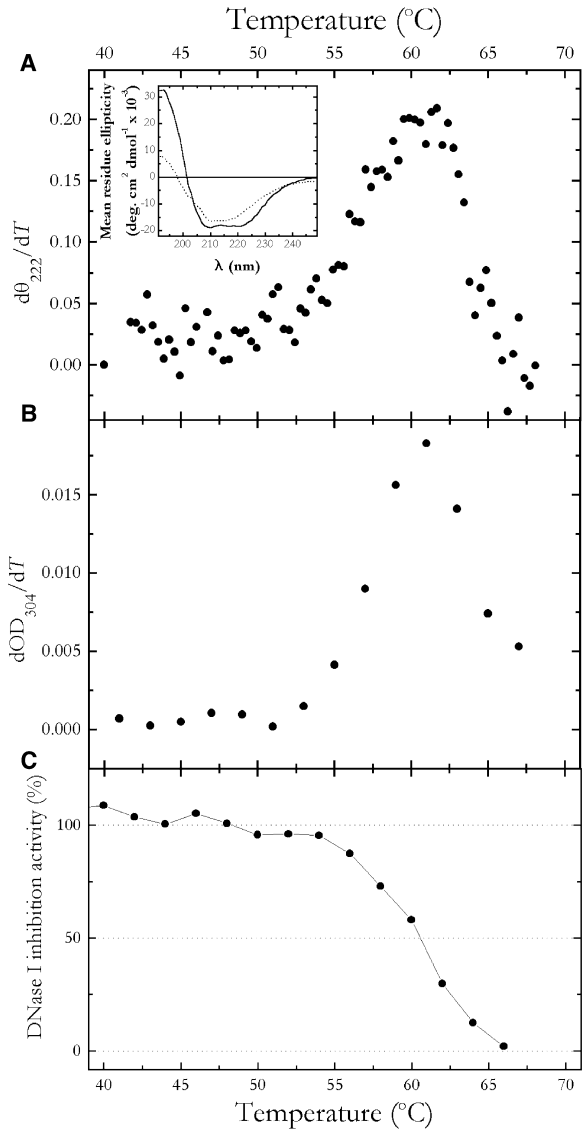

Fig. 2. Thermal melting profiles of monomeric β/γ-Ca-ATP-actin, assessed with three different methods. (A) Temperature-dependent change in ellipticity at 222 nm (θ_{222}) of an actin solution, determined by CD spectroscopy. Inset: spectra of native and heat-denatured actin (solid and broken lines, respectively). (B) Temperature-dependent change in absorbance at 304 nm (D_{304}). (c) Heat-induced loss of DNase I-binding capacity. All three methods gave a T_m of 60.5–61.0 °C for this particular preparation of actin.

indicates a more cooperative unfolding. However, a is only meaningful for internal comparison and should not be confused with the cooperativity index derived from Hill plots.

The energy of activation (E_a) for an irreversible unfolding reaction can be determined from the heating-rate dependence of T_m using:

$$\ln\left(\frac{v}{T_m^2}\right) = C - \frac{-E_a}{RT}$$

where v is the heating rate and C is a constant [39]. Consequently E_a can be estimated from the slope of:

$$\ln\left(\frac{v}{T_m^2}\right) \text{ vs. } \frac{1}{T_m}$$

Here, E_a was estimated from thermal transitions recorded with heating rates of 20, 30, 40, 60, and 90 °C·h^{-1}.

Unfolding kinetics

To determine the kinetics of the thermal inactivation of G-actin, samples were incubated at elevated temperatures, and aliquots were removed at intervals and analysed for DNase I-inhibition activity as described above. The fraction of active actin remaining (f_{nat}) was plotted as a function of time, and the apparent denaturation rate constant (k_{app}) was determined by curve fitting to:

$$f_{nat} = e^{k_{app} \cdot t}$$

using Microcal ORIGIN. The k_{app} values for several temperatures were plotted in Arrhenius plots from which the energy of activation (E_a) and the frequency factor (A) were estimated.

CD spectropolarimetry

CD spectra of actin (8 μM in buffer G) were recorded on a Jasco J-720 spectropolarimeter, using 0.1 mm-cuvettes. To monitor the thermal unfolding of actin, the ellipticity at 222 nm was recorded while the protein solution was heated at a rate of 40 °C·h^{-1} using a Peltier-type thermostatic cell holder (Jasco PTC-343) and 1-mm cuvettes.

Ultraviolet difference spectroscopy

Difference spectra of native and heat-denatured G-actin (recorded on a Hewlett-Packard 8452A spectrophotometer) showed a maximum at 304 nm, in agreement with a previous study [20]. Thermal unfolding was followed by heating samples at a rate of 40 °C·h^{-1} and monitoring the D_{304} against a reference sample at 25 °C.

Solvent-accessible surface areas

Solvent-accessible surface areas were calculated using the program NACCESS (S. J. Hubbard & J. M. Thornton, Department of Biochemistry and Molecular Biology, University College, London, 1993).

RESULTS

The DNase I-inhibition assay for studies of thermal unfolding of G-actin

Analysis of native and heat-inactivated monomeric β/γ-actin with Ca-ATP by CD spectropolarimetry showed that approximately 30% of the α-helical structure was lost after thermal unfolding (Fig. 2A, inset). This is similar to results obtained for skeletal muscle, gizzard, and yeast actins [4,19,23]. The change in ellipticity at 222 nm and in optical density at 304 nm showed that the actin denatured with a T_m of 60.5–61.0 °C when heated at a rate of 40 °C·h^{-1} (Fig. 2). Similarly, with the DNase I-inhibition assay, a single transition with a T_m of 60.5 °C was observed using the same heating rate and solution conditions. Thus, the loss of DNase I-inhibition activity during heat treatment coincided with the unfolding of the secondary structure of actin as observed by CD spectropolarimetry and difference spectroscopy, which indicates that the DNase I-inhibition assay can be used to monitor the thermal unfolding of actin. The reproducibility of the DNase I-inhibition assay was demonstrated by the low variation in the

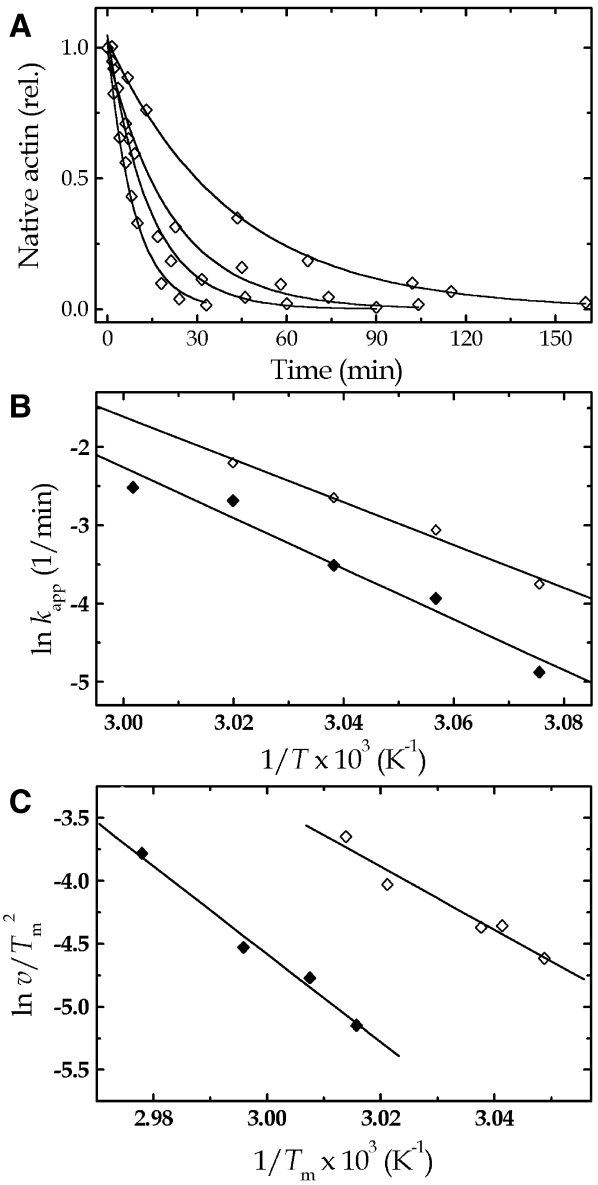

Fig. 3. Irreversible unfolding of monomeric skeletal muscle α-actin. (A) Loss of DNase I-inhibition activity of Mg-ATPactin incubated at (from left to right) 58, 56, 54, and 52 °C. The trend-lines represent best fits using a first-order expression. (B) Arrhenius plot of the apparent unfolding rate constants for actin with bound Mg-ATP (◇) or Ca-ATP (◆). (C) Modified Arrhenius plot of the heating-rate dependence of T_m for actin with bound Mg-ATP or Ca-ATP (symbols as in B). Both methods (B and C) yielded similar estimates of the activation energy (E_a) and Arrhenius factor for the thermal unfolding reaction (see Table 1).

T_m values determined for different preparations of β/γ-Ca-ATP-actin (SD = 0.7 °C; n = 6). For skeletal muscle actin a T_m of 60.5 °C was determined here, which is consistent with values determined previously using microcalorimetry, CD spectropolarimetry, and fluorescence spectroscopy [4,23–25].

Irreversible unfolding of G-actin

Following thermal inactivation, DNase I-inhibition could not be regained by incubation of the actin either at room temperature or at 4 °C. The midpoints of the transitions from the active to inactive state showed a strong dependence on the heating rate, indicating that the thermal denaturation of G-actin is not a thermodynamic equilibrium process (e.g. [39]). Furthermore, when G-actin solutions were incubated at constant temperatures, equilibria between active and inactive actin were not established. Instead the samples lost their DNase I-binding capacity completely with apparent first-order kinetics (Fig. 3A), These results suggest the following scheme for the thermal unfolding of G-actin:

$$N \xrightarrow{k_{app}} D$$

Where N is native actin, and k_{app} is a temperature-dependent, apparent first-order rate constant. D denotes partially denatured actin, which has lost DNase I-binding capacity but retains approximately 70% of its α-helical structure. Equilibrium thermodynamic analysis is frequently applied to irreversible protein denaturation under the assumption that the N → D transition is divided into reversible formation of an intermediate

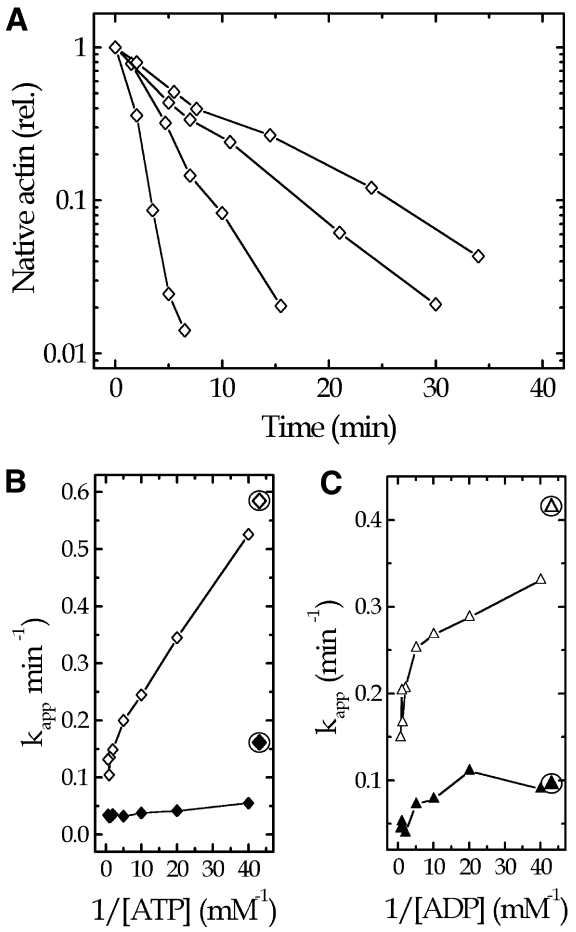

Fig. 4. Effect of ATP concentration on the apparent unfolding rate of monomeric β/γ-actin. (A) Semi-logarithmic plot illustrating the time course of the loss of DNase I-binding capacity in Mg-actin (6 μM) incubated at 55 °C with different concentrations of free ATP (from left to right: 0, 0.1, 0.5, and 1.0 mM). From this and similar experiments, the apparent first-order unfolding rate constants (k_{app}) were determined. (B) Dependence of the k_{app} at 55 °C on the concentration of free ATP. □, Mg-ATP-actin; ■, Ca-ATP-actin. (C) Dependence of the k_{app} at 50 °C on the concentration of free ADP. △, Mg-ADP-actin; ▲, Ca-ADP-actin. The circled values for k_{app} in panels (B) and (C) represent the values determined in absence of excess nucleotide.

(I) followed by irreversible denaturation of this intermediate at higher temperatures:

$$N \leftrightarrow I \rightarrow D$$

In Fig. 4, it is shown that the apparent first-order unfolding rate constants for β/γ-actin were a function of the concentration of free nucleotide and depended on the divalent cation bound to the actin. This suggests the existence of a nucleotide-free intermediate, which either can be stabilized by rebinding nucleotide (*nuc*), or unfolds spontaneously with first-order kinetics:

$$N{\cdot}nuc \leftrightarrow I + nuc \rightarrow D$$

Scheme 1

The good fit of the experimental data to first-order kinetics (Figs 2A and 3A) and the dependence of the transition temperature on the heating rate (Fig. 3C) indicate that the unfolding reaction is dominated by the kinetics of the irreversible step [39–43]. Under these conditions, the intermediate never accumulates, and only the N and D states are significantly populated. Therefore, the thermal unfolding of G-actin should be considered irreversible [43,44], and cannot be treated as an equilibrium-thermodynamic process (e.g. [23]).

Actin was stabilized by excess nucleotide under all conditions studied (Fig. 4). A fourfold excess of ATP reduced the apparent unfolding rate of Ca-ATP-actin (6 μM) by a factor of approximately three, but at higher concentrations of free ATP the stabilizing effect increased only slightly. In the case of Ca-ADP-actin, stabilization was not observed unless the concentration of free ADP exceeded 0.5 mM. The apparent unfolding rate was then reduced by a factor of two to three. With Mg-actin, the stabilizing effect of free nucleotide was even more pronounced. At 1.5 mM free ATP, the unfolding rate was six times slower than in the absence of free ATP.

Stabilization of carboxypeptidase B by Zn^{2+} during thermal denaturation has been described by a kinetic model [39]. Applying this model to the stabilization of actin by nucleotide led to:

$$D + nuc \overset{k_N}{\leftarrow} N{\cdot}nuc \overset{K}{\leftrightarrow} I + nuc \overset{k_I}{\rightarrow} D$$

Scheme 2

where k_N and k_I are the rate constants for unfolding from the native state and denaturation of the nucleotide-free intermediate, respectively, and K is the equilibrium constant for nucleotide binding. This scheme differs from Scheme 1 by the addition of an irreversible step accounting for denaturation of actin with bound nucleotide. The formation of the denatured state can be described by:

$$\frac{d[D]}{dt} = k_N{\cdot}[N{\cdot}nuc] + k_I[I]$$

Scheme 3

The equilibrium constant for nucleotide binding is defined as:

$$K = \frac{[I]{\cdot}[nuc]}{[N{\cdot}nuc]}$$

Scheme 3 can therefore be written in the form:

$$\frac{d[D]}{dt} = [N{\cdot}nuc]{\cdot}\left(k_N + {\cdot}\frac{k_I{\cdot}K}{[nuc]}\right)$$

Scheme 4

Under the assumption that the nucleotide-free intermediate I can inhibit DNase I, the apparent first-order denaturation rate constant is given by:

$$k_{app} = \left(k_N + {\cdot}\frac{k_I{\cdot}K}{[nuc]}\right)$$

Thus, the curves of k_{app} vs. [nucleotide]$^{-1}$ (Fig. 4B,C) have slopes of $k_I{\cdot}K$ and an ordinate intercept of k_N. For Ca-actin these curves were linear, but in the case of Mg-actin they consisted of two linear phases. Under all four experimental conditions, the values of k_N determined by extrapolation were very low, suggesting that actin denatured mainly via the nucleotide-free intermediate, corroborating Scheme 1 for the thermal unfolding.

Kinetic parameters for the irreversible thermal denaturation of G-actin

The activation energies (E_a) for the irreversible unfolding reactions were estimated either from the dependence of the melting temperatures on the heating-rate, or from Arrhenius plots of the temperature dependence on the apparent denaturation rate (Fig. 3). For the unfolding reaction of α-Ca-ATP-actin, E_a values of 269 ± 31 and 290 ± 25 kJ·mol^{-1}, and frequency factors of 95 and 100 were estimated with these two methods, respectively (Table 1). These results are in good agreement with a recent determination of these parameters [25], lending further credence to the validity of the DNase I-inhibition assay for studies of actin unfolding.

Effects of nucleotide and divalent cation

The bound nucleotide and high-affinity divalent cation were found to determine the thermal stability of β/γ-actin to a large extent. The ATP-actin was more stable than ADP-actin, regardless of whether Mg^{2+} or Ca^{2+} was bound (Fig. 5 and Table 1). As judged from the higher slopes of the transitions seen with ATP-actin, the unfolding was more cooperative in this case, confirming the importance of the γ-phosphate of ATP for interdomain coupling [6]. With Mg^{2+} replacing Ca^{2+} at the high-affinity binding site, the T_m were lowered by 4–5 °C with both ATP-and ADP-actin. This reduction in stability may be explained by the lower affinity of actin for Mg^{2+} than for Ca^{2+}. A comparison of the unfolding activation energies for the ATP-and ADP-actins revealed that E_a for Mg-actin was not

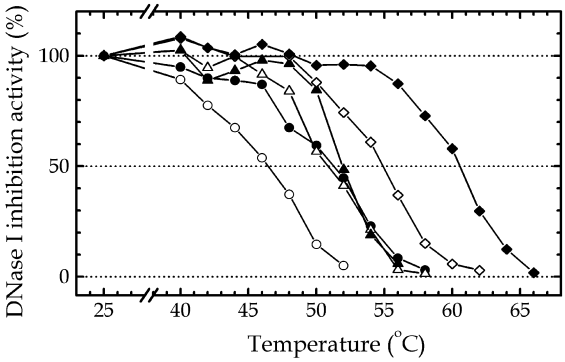

Fig. 5. Effect of the state of nucleotide hydrolysis on the temperature-dependent loss of DNase I-inhibition activity of monomeric β/γ-actin. Open symbols, Mg-actins; filled symbols, Ca-actins; circles, ADP-actin; triangles, ADP.P_i-actin; diamonds, ATP-actin. T_m values are summarized in Table 1.

Table 1. Thermal stability of monomeric actin, determined by the DNase I-inhibition assay. A comparison of different actin isoforms, and the effects of various ligands. Sources of actin: rabbit skeletal muscle (denoted α), bovine thymus (β and γ), and *Saccharomyces cerevisiae* (denoted yeast). The T_m and slopes of the melting curves (*a*) are from transitions recorded with a heating rate of 40 °C·h^{-1}. The values represent single determinations or, where SD are presented, the means of three or more determinations. The activation energy (E_a) and Arrhenius factor (*A*) were determined by analysis of the heating-rate dependence of the melting temperatures and, in the case of α-actin, also of the apparent denaturation rate constants at different temperatures (second value). Conditions, G-buffer with either ADP or ATP, unless stated otherwise (see Materials and methods for further details).

Isoform	Ligands	T_m (°C)	*a*	E_a (kJ·mol^{-1})	*A*
α	Ca-ATP	60.4 ± 0.3	10.5 ± 0.3	291 ± 25/269 ± 31	100/95
α	Mg-ATP	56.0 ± 0.3	9.7 ± 0.1	208 ± 26/227 ± 19	72/80
β	Ca-ATP	58.2 ± 0.6	12.3 ± 2.1		
β	Mg-ATP	52.8 ± 1.2	9.7 ± 0.6	205 ± 25	73
γ	Ca-ATP	60.1 ± 0.8	12.1 ± 0.9		
γ	Mg-ATP	55.6 ± 0.5	10.9 ± 1.1	268 ± 52	94
yeast	Ca-ATP	59.3 ± 1.0	11.7 ± 0.9		
yeast	Mg-ATP	55.2 ± 0.9	10.9 ± 0.9	211 ± 10	73
β/γ	Ca-ATP	60.1 ± 0.7	10.3 ± 0.8	283 ± 17[c]	95
β/γ	Mg-ATP	56.8 ± 2.5	9.3 ± 1.2	228 ± 41[d]	79
β/γ	Ca-ADP	51.7 ± 0.5	8.4 ± 1.4	214 ± 23	87
β/γ	Mg-ADP	46.4 ± 0.6	8.6 ± 0.6	247 ± 47	77
β/γ	Ca-ADP.P_i [a]	52.5	12.3		
β/γ	Mg-ADP.P_i [a]	51.0	10.2		
β/γ	Ca-ADP.V_i [b]	52.5	9.3		
β/γ	Mg-ADP.V_i [b]	47.0	9.5		
β/γ	Ca-ADP + AlF_4	53.0	9.9		
β/γ	Mg-ADP + AlF_4	50.0	12.1		
β/γ	Ca-ADP + BeF_x	51.5	9.2		
β/γ	Mg-ADP + BeF_x	46.5	9.4		
β/γ	Ca-ATP + profilin	56.5	10.5		
β/γ	Mg-ATP + profilin	53.0	8.6		
β/γ	Ca-ADP + profilin	54.5	10.1		
β/γ	Mg-ADP + profilin	49.0	12.2		

[a] Prepared from ADP.P_i-F-actin; [b] prepared from ADP.V_i-F-actin; [c] E_a = 81 ± 20 kJ mol^{-1} in the abscence of excess ATP; [d] E_a = 151 ± 19 kJ·mol^{-1} in the abscence of excess ATP.

significantly affected by the presence of the γ-phosphate group, whereas the value for Ca-actin was 70 kJ·mol^{-1} higher with ATP than with ADP (Table 1). The observations with the Mg-actin illustrate that T_m and E_a are different measures of protein stability. The T_m value is empirical, whereas E_a is an enthalpy influenced by both the kinetics and midpoint of the transition.

When inorganic phosphate (P_i; 0.5 or 5 mM) was added directly to ADP-actin, no effect on the T_m was observed (data not shown). Vanadate (V_i; 1 mM) had a slightly stabilizing effect. However, when monomeric ADP.P_i-actin was prepared by depolymerizing F-actin in ADP and P_i (10 mM), the presence of the inorganic phosphate stabilized the protein and conferred a higher degree of cooperativity to the unfolding reactions (Fig. 5 and Table 1). This suggests that the release of P_i from actin monomers results in a conformational change which prevents rebinding of P_i and causes an irreversible loss of interdomain coupling. Addition of AlF_4, but not BeF_x, to monomeric ADP-actin raised both its T_m and the degree of unfolding cooperativity. These effects of inorganic phosphate and phosphate analogs were seen with either Mg^{2+} or Ca^{2+} present at the high-affinity divalent cation binding site.

The difference in the unfolding activation energies in the presence and absence of bound ATP (E_{aG} and E_{a0}, respectively) reflects the enthalpy of nucleotide binding (H_{ATP}) according to $E_{aG} = E_{a0} - H_{ATP}$. The unfolding energies of ATP-actin free of excess nucleotide (E_{a0}) were lower than in the presence of 0.5 mM free ATP (E_{aG}). This difference was considerably larger for Ca- than for Mg-actin (Table 1). Under the assumption that the concentration of actin with bound nucleotide was negligible during unfolding in the absence of excess ATP (see Scheme I), H_{ATP} was estimated to 80 kJ·mol^{-1} in Mg-actin and to 200 kJ·mol^{-1} in Ca-actin. These results are in agreement with a tighter binding of Ca-ATP compared with Mg-ATP, and the values are in the same range as the binding energies determined for other protein–ligand interactions [16].

Isoform comparison

Table 1 shows the T_m values for different actin isoforms. Rabbit skeletal muscle α-actin and bovine thymus γ-actin had similar stabilities, whereas β-actin, prepared either from bovine thymus or expressed in yeast (see [6]), was inactivated at lower temperatures. Yeast actin was more stable than β-actin but less stable than the α- and γ-isoforms. Exchanging the high-affinity Ca^{2+} for Mg^{2+} led to a 4–5 °C decrease in the T_m for α-, β- and γ-actin. A similar decrease was also observed with yeast actin.

Effect of profilin on the thermal stability of β/γ-actin

A fourfold excess of profilin over actin did not affect the affinity of the DNase I–actin complex (data not shown). Thus, it is possible to use the DNase I-inhibition assay to study the

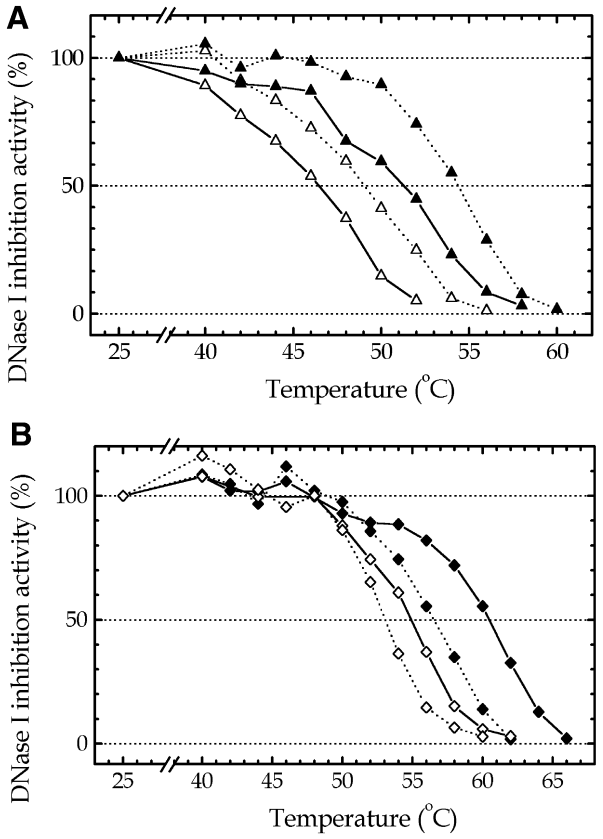

Fig. 6. The effects of equimolar amounts of profilin on the thermal stability of β/γ-actin. Melting curves for either ADP-actin (A) or ATP-actin (B). Open symbols, Mg-actin; filled symbols, Ca-actin; solid lines, actin alone; broken lines, in presence of profilin. T_m values are summarized in Table 1.

effect of profilin on actin unfolding. The presence of equimolar profilin decreased the thermal stability of ATP-actin regardless of whether Mg^{2+} or Ca^{2+} were bound and did not affect the cooperativity of the reaction (Fig. 6, Table 1). Profilin, however, markedly stabilized ADP-actin against thermal unfolding, raising the unfolding cooperativity. Thus, dependent on the status of the actin-bound nucleotide, profilin either destabilized or stabilized G-actin. Similar results were obtained in the presence of Mg^{2+} or Ca^{2+}.

Effect of phalloidin

The presence of phalloidin up to a 10-fold excess over actin under non-polymerizing conditions did not change the DNase I-inhibiting activity of actin, enabling a study of the effect of phalloidin on thermal unfolding of G-actin. Also in these experiments, the concentrations of monomeric β/γ-actin were low enough to prevent heat-induced filament formation. The results showed that the thermal transitions of 1 μM Ca-ATP-actin in the absence of phalloidin, or in the presence of either equimolar or a 10-fold molar excess of phalloidin were identical, demonstrating that phalloidin had no stabilizing effect on G-actin.

DISCUSSION

The interaction between DNase I and the DNase I-binding loop (residues 38–51) in subdomain 2 of actin (Fig. 1) buries 812 $Å^2$ of solvent-accessible surface area of actin. The site on subdomain 4 is less extensive (156 $Å^2$), but important, as it includes a salt bridge (DNase I His44, actin Glu207) and a hydrogen bond (DNase I Gln13, actin Thr203) [2]. In the crystal complexes of gelsolin–actin and profilin–actin, the DNase I-binding loop is one of the least ordered regions of the molecule [45–47]. The existence of linkages between subdomain 2 and other parts of the molecule is known from solution studies [48–51]. Formal analysis of domain motions in actin using the four available actin structures [52] indicated that subdomain 2 rotates relatively independently of the rest of the small domain of actin (i.e. subdomain 1), and small changes in the structure of subdomain 2 probably explain the small condition-dependent variations in the DNase I-inhibiting activity observed (data not shown).

During time- and temperature-dependent thermal unfolding, 30% of the α-helicity was lost in a process that coincided with a loss in DNase I-inhibiting activity, suggesting that these processes are closely linked. As 44% of the amino acid residues in actin are found in α-helices (166 of 375 residues), and only eight of these residues reside in subdomain 2 (56–60 and 62–64), it is concluded that binding of DNase I to actin not only probes the status of subdomain 2, but the status of the overall three-dimensional fold of actin.

The fold of actin is rather intricate, with subdomains that are not formed from contiguous stretches of the polypeptide, i.e. actin is not a segmented protein. Instead the chain, starting from the N-terminus, transverses the subdomains in the order 1→2→1→3→4→3→1, creating a small and a large domain (subdomains 1 + 2 and 3 + 4, respectively) connected by two crossed helices at the bottom of the interdomain cleft. Thus, changes in any part of the structure may be communicated throughout the molecule *via* the interdomain linkages [47], and it is not surprising that conformational changes in subdomain 2 can be caused by those occurring in subdomains 1 and 3, where most of the α-helices are found. As the DNase I-binding site is located far away from the interdomain hinge and shear regions, its conformation will be sensitive even to small conformational changes affecting the interdomain angle, resulting in measurable changes in the DNase I-binding activity. The DNase I-inhibition assay is simple, rapid and sensitive, requiring only a single beam UV-spectrophotometer, and therefore should prove useful for studies on unfolding and refolding of actin.

It is known from earlier studies that a 30–40% loss in the α-helix content of actin occurs with a T_m of between 55 and 60 °C, and that no additional changes take place if the protein is further heated to 95 °C. This structural transformation corresponds to the initial phase in the unfolding of actin that occurs at moderate concentrations of the chaotropic agent guanidinium chloride, or after addition of chelating agents removing the high-affinity divalent cation (and consequently the actin-bound nucleotide). This process is irreversible unless chaperonins are present. The further transformation of the protein to the fully denatured state that occurs at higher concentrations of guanidinium chloride appears to be reversible.

G-actin treated with EDTA denatures with first-order kinetics [4,12], and G-actin loses its high-affinity divalent cation and nucleotide upon heat treatment [4]. Thus both EDTA- and heat-induced denaturation of G-actin occur by irreversible unfolding after reversible loss of the nucleotide–cation complex, as described by a three-state model (Scheme 1). The implication for chaperonin-mediated actin folding [17] is that a partially folded, nucleotide-free precursor of actin must be stabilized to form a conformation that is competent to bind nucleotide,

before isomerization to the native form can occur. Actin, with its high abundance and well-established biochemistry, should be an ideal model protein to study the final stages of folding. The DNase I-inhibition assay, with its high specificity for the native conformation of actin and a detection limit in the range of 0.1 μg, should be useful in such studies. Commonly used polymerization assays rely on carrier actin, and involve the risk of coaggregation of partly denatured actin.

Many proteins with complex structure (with or without ligands bound) unfold irreversibly during heat treatment into partially folded structures. In such cases, the thermal denaturation cannot be analysed using models that depend on the establishment of thermodynamic equilibria. Instead, kinetic models have to be used [39–43,53–62]. The present analysis confirms that the T_m values of muscle and nonmuscle G-actins depend on the heating rate, that the thermal unfolding proceeds with first-order kinetics, and that it is an irreversible process (Scheme 1) [4,19,23,25,28]. This warrants determination of E_a, but not of ΔG, as done in some studies [23]. The activation energies for the thermal unfolding of actin were of similar magnitude as those determined for other proteins [60], and considering that the loss of secondary structure in actin is limited, the activation energies obtained are in reasonable agreement with the theoretical value of 4 kJ per mol of unfolded residue [63].

The strong dependence of the unfolding kinetics on the nucleotide concentration observed here (Fig. 4) argues against side reactions such as polymerization, disulfide formation, and proline isomerization, as the cause of irreversibility [22]. Given the considerable difference in the stabilities of ADP-and ATP-actin (Table 1), discrepancies in the literature on actin stability may be explained by differences in the relative amounts of ATP and ADP available per actin molecule.

Effect of nucleotide and cation

The importance of the γ-phosphate and residues in the two phosphate-binding loops for interdomain coupling indicated in the actin structure [2] was demonstrated by analyses of actin mutants [6]. As shown here, monomeric ADP-actin was less thermostable than both ATP-actin and ADP-actin with the γ-phosphate position occupied by either inorganic phosphate or phosphate analogs. This is consistent with the binding energy of a ligand being directly related to its stabilizing effect [64]. The ADP-actin was stabilized by AlF_4 to a greater extent than by inorganic phosphate, vanadate, or BeF_x, and the stabilizing effect on the Mg-form was more pronounced than on the Ca-form of the protein. Thus, AlF_4 probably makes the most extensive contacts with the protein, which is consonant with the finding that, of all the ligands tested, ADP·AlF_4 conferred the highest degree of cooperativity to the unfolding reactions. The unfolding characteristics of ADP·AlF_4-actin were closer to those of ATP-actin than of ADP-actin, in particular with the hydrolytically active Mg-form of the protein. This implies that ADP·AlF_4 with its interactions with actin might resemble the transition state in the hydrolysis reaction, as in a number of phosphoryl transferases (reviewed in [65]).

The kinetic analysis of the effect of free nucleotide on actin unfolding showed that even though the nucleotide-free intermediate does not accumulate during thermal unfolding of actin, the reaction proceeded according to Scheme 1. This scheme for actin unfolding has been proposed before based on inactivation of actin, as determined by the inability of nucleotide-free actin to polymerize [3,4] or to rebind nucleotide [66]. The apparent unfolding rates obtained in these studies and those presented here show that the loss of bound nucleotide first leads to inability to rebind nucleotide, then to loss of polymerizability, and finally to more extensive losses of secondary structure and DNase I-binding capacity. This order of events is also confirmed by the faster loss of polymerizability than α-helix content during thermal unfolding [4].

The unfolding kinetics of G-actin were affected by excess nucleotide in such a way that the plots of the rate constant for unfolding (k_{app}) against the inverse of the nucleotide concentration ([nucleotide]$^{-1}$) were linear for CaATP-actin (Fig. 4B). In the case of MgATP-actin, two linear segments with different slopes were observed. The steeper slope at higher concentrations of ATP may reflect a low affinity binding of ATP protecting the actin against thermal denaturation. Evidence for a second nucleotide-binding site has been reported earlier [67]. Interaction at this site influenced nucleotide exchange at the high affinity site, and appeared not to be due to chelation of divalent cations. Our observations corroborate this finding in that the stabilizing effect of nucleotide increased at high concentrations, whereas chelation of divalent cation by excess nucleotide would have destabilized the actin.

The observation that Mg-actin was less thermostable than Ca-actin is consistent with the view that MgATP is less firmly bound to the actin than CaATP (reviewed in [68]). This was also suggested by molecular dynamic simulation studies [69] which indicated a more open conformation of Mg-actin than of Ca-actin. The present study shows that there was no difference in the activation energies for ADP-and ATP-actin unless Ca^{2+} was bound. Thus in Mg-actin, the loss of the γ-phosphate seems to be compensated for by formation of additional bonds to ADP. Consistent with this, ATP binds 4- to 12-fold more tightly than ADP to Mg-actin, while the difference in affinities is nearly 200-fold with Ca-actin (reviewed in [68]),

Isoform differences

The thermostabilities of the different actins studied here were affected by exchange of nucleotide and cation to the same degrees. This shows that the nature of the nucleotide–cation complex is a stronger determinant of actin stability than isoform differences. Despite the conserved nature of the nucleotide–cation binding site, cytoplasmic β-actin was less heat-stable than skeletal muscle α-actin, cytoplasmic γ-actin and yeast actin. The difference in stability between the β- and γ-actins was surprising, as these isoforms differ only in their N-terminal sequences (D_2, D_3, D_4…V_{10} for β-actin, E_2, E_3, E_4…I_{10} for γ-actin). The implication is that the properties of the N-terminus influence the stability of the protein through its interactions with other regions of the molecule. Comparison of heat- and EDTA-induced inactivation of smooth and striated muscle actins led to the suggestion that residues 17 and/or 89, but not the composition of the N-terminus, influenced actin stability [4]. The β- and γ-nonmuscle isoforms studied here as well as yeast actin are identical at positions 17 and 89, whereas they differ from skeletal muscle α-actin at these positions. However, these four actins do not separate into two groups with respect to their stability. Instead, β-actin is the least stable and γ-actin is as stable as α-actin. In addition, yeast actin, which is the most divergent of the actins studied here and the one with the most basic N-terminus, has an intermediate thermal stability. Thus clearly, the composition of the N-terminus does affect actin stability, but it is difficult to predict the effects of specific amino acid replacements in this context.

Effects of profilin

Profilin is known to facilitate the exchange of actin-bound ATP [70] and inhibit the ATPase activity of the protein [71]. In the present experiments, profilin destabilized ATP-actin, in agreement with a profilin-induced cleft-opening [47]. However, when ADP was bound, profilin stabilized the actin and markedly raised the unfolding cooperativity, suggesting a profilin-induced tighter binding of ADP to actin. It has been shown that profilin reduces the affinity of actin for MgADP by promoting MgADP dissociation and inhibiting MgADP association [72]. Therefore, profilin might fix the interdomain angle in ADP-actin, trapping the molecule in a more stable conformation.

Phalloidin has been shown to stabilize filamentous actin against heat denaturation [24,73]. It has been proposed that phalloidin also stabilizes monomeric actin [24,26], implying phalloidin binding to G-actin. However, no effect of phalloidin on the thermal stability of G-actin was found here, possibly because the low concentrations of actin prevented uncontrolled heat-induced polymerization. Thus, the DNase I-inhibition assay, due to its high sensitivity, enables the study of thermal stability of G-actin under polymerizing conditions, e.g. in the presence of Mg^{2+}, excess of P_i or phosphate analogs, or of phalloidin.

CONCLUSION

It is possible that chaperonin-mediated actin folding *in vivo* [17] occurs by the stabilization of nucleotide-free actin in a conformation that allows nucleotide-binding and subsequent folding to the native state. The nucleotide-free intermediate proposed in Scheme I may represent such a precursor of native actin, and a characterization of this short-lived intermediate by appropriate techniques (e.g. stopped flow analysis) would be of great interest. It is well known that cooperativity between secondary structural elements plays an important role in folding (reviewed in [14–16]), and the cooperative interdomain relationship addressed here and in previous studies ([74] and references therein) is therefore expected to be crucial also to the folding of actin.

ACKNOWLEDGEMENTS

We thank G. Eriksson for making the CD polarimeter available to us and P. Dahlberg for assistance in its use, R. Page for calculating solvent-accessible surface areas, R. L. Baldwin and T. Nyman for valuable discussions, and G. D. Bowman, I. M. Nodelman and R. Page for comments on the manuscript. Finally, we acknowledge financial support from the Swedish National Science Research Council (NFR) to U. L. and R. K., and to C. E. S. from the NIH (GM44038).

REFERENCES

1. Rubenstein, P.A. (1995) The functional importance of multiple actin isoforms. *Bioessays* **12**, 309–315.
2. Kabsch, W., Mannherz, H.G., Suck, D., Pai, E.F. & Holmes, K.C. (1990) Atomic structure of the actin: DNase I complex. *Nature* **347**, 37–44.
3. Asakura, S. (1961) The interaction between G-actin and ATP. *Arch. Biochem. Biophys.* **92**, 140–149.
4. Strzelecka-Golaszewska, H., Venyaminov, S.Y., Zmorzynski, S. & Mossakowska, M. (1985) Effects of various amino acid replacements on the conformational stability of G-actin. *Eur. J. Biochem.* **147**, 331–342.
5. Mannherz, H.G., Goody, R.S., Konrad, M. & Nowak, E. (1980) The interaction of bovine pancreatic deoxyribonuclease I and skeletal muscle actin. *Eur. J. Biochem.* **104**, 367–379.
6. Schüler, H., Korenbaum, E., Schutt, C.E., Lindberg, U. & Karlsson, R. (1999) Mutational analysis of serine 14 and aspartic acid 157 in the nucleotide-binding site of β-actin. *Eur. J. Biochem.* **265**, 210–220.
7. Lindberg, U. (1967) Studies on the complex formation between deoxyribonuclease I and spleen inhibitor II. *Biochemistry* **6**, 343–347.
8. Lazarides, E. & Lindberg, U. (1974) Actin is the naturally occurring inhibitor of deoxyribonuclease I. *Proc. Natl Acad. Sci. USA* **71**, 4742–4746.
9. Blikstad, I., Markey, F., Carlsson, L., Persson, T. & Lindberg, U. (1978) Selective assay of monomeric and filamentous actin in cell extracts, using inhibition of deoxyribonuclease I. *Cell* **15**, 935–943.
10. Carlsson, L., Markey, F., Blikstad, I., Persson, T. & Lindberg, U. (1979) Reorganization of actin in platelets stimulated by thrombin as measured by the DNase I-inhibition assay. *Proc. Natl Acad. Sci. USA* **76**, 6376–6380.
11. Blikstad, I. & Carlsson, L. (1982) On the dynamics of the microfilament system in HeLa cells. *J. Biol. Chem.* **93**, 122–128.
12. Hayden, S.M., Miller, P.S., Brauweiler, A. & Bamburg, J.R. (1993) Analysis of the interactions of actin depolymerizing factor with G- and F-actin. *Biochemistry* **32**, 9994–10004.
13. Ikeuchi, Y., Iwamura, K. & Suzuki, A. (1991) Estimation of denaturation of actin in the actin-myosin complex treated with various conditions by DNAase I inhibition assay. *Int. J. Biochem.* **23**, 985–989.
14. Creighton, T.E. (1995) Protein folding: an unfolding story. *Curr. Biol.* **5**, 353–356.
15. Shakhnovich, E.I. (1999) Folding by association. *Nat. Struct. Biol.* **6**, 99–102.
16. Fersht, A. (1999) *Structure and Mechanism in Protein Science.* Freeman, New York.
17. Vainberg, I.E., Lewis, S.A., Rommelaere, H., Ampe, C., Vandekerckhove, J., Klein, H.L. & Cowan, N.J. (1998) Prefoldin, a chaperone that delivers unfolded proteins to cytosolic chaperonin. *Cell* **93**, 863–873.
18. Willison, K. (1998) Composition and function of the eukaryotic cytosolic chaperonin-containing TCP-1. In *Molecular Chaperones and Folding Catalysts* (Bukau, B., ed.), pp. 555–573. Harwood Academic Publishers, London.
19. Nagy, B. & Strzelecka-Golaszewska, H. (1972) Optical rotatory dispersion and circular dichroic spectra of G-actin. *Arch. Biochem. Biophys.* **150**, 428–435.
20. Contaxis, C.C., Bigelow, C.C. & Zarkadas, C.G. (1977) The thermal denaturation of bovine cardiac G-actin. *Can. J. Biochem.* **55**, 325–331.
21. Anderson, N.L. (1979) The β and γ cytoplasmic actins are differentially thermostabilized by MgADP; γ actin binds MgADP more strongly. *Biochem. Biophys. Res. Comm.* **89**, 486–490.
22. Tatunashvili, L.V. & Privalov, P.L. (1984) Calorimetric study of G-actin denaturation. *Biofizika* **29**, 583–585.
23. Bertazzon, A., Tian, G.H., Lamblin, A. & Tsong, T.Y. (1990) Enthalpic and entropic contributions to actin stability: calorimetry, circular dichroism, and fluorescence study and effects of calcium. *Biochemistry* **29**, 291–298.
24. Le Bihan, T. & Gicquaud, C. (1991) Stabilization of actin by phalloidin: a differential scanning calorimetric study. *Biochem. Biophys. Res. Comm.* **181**, 542–547.
25. Le Bihan, T. & Gicquaud, C. (1993) Kinetic study of the thermal denaturation of G actin using differential scanning calorimetry and intrinsic fluorescence spectroscopy. *Biochem. Biophys. Res. Comm.* **194**, 1065–1073.
26. Vedenkina, N.S., Kalinichenko, L.P. & Permyakov, E.A. (1995) The effect of phalloidin on the stability of F- and G-actin. *Mol. Biol. Moskva* **29**, 349–352.
27. Chen, X., Peng, J., Pedram, M., Swenson, C.E. & Rubenstein,

P.A. (1995) The effect of the S14A mutation on the conformation and thermostability of *Saccharomyces cerevisiae* G-actin and its interaction with adenine nucleotides. *J. Biol. Chem.* **270**, 11415–11423.

28. Turoverov, K.K., Biktashev, A.G., Khaitlina, S. & Yu. & Kuznetsova, I.M. (1999) The structure and dynamics of partially folded actin. *Biochemistry* **38**, 6261–6269.
29. Lindberg, U., Schutt, C.E., Hellsten, E., Tjäder, A.-C. & Hult, T. (1988) The use of poly (L-proline)-sepharose in the isolation of profilin and profilactin complexes. *Biochim. Biophys. Acta* **967**, 391–400.
30. Segura, M. & Lindberg, U. (1984) Separation of non-muscle isoactins in the free form or as profilactin complexes. *J. Biol. Chem.* **259**, 3949–3954.
31. Pardee, J.D. & Spudich, J.A. (1982) Purification of muscle actin. *Methods Enzymol.* **85**, 164–181.
32. Karlsson, R. (1988) Expression of chicken beta-actin in *Saccharomyces cerevisiae*. *Gene* **68**, 249–257.
33. Houk, T.W. & Ue, K. (1974) The measurement of actin concentration in solution: a comparison of methods. *Anal. Biochem.* **62**, 66–74.
34. Gershman, L.C., Newman, J., Selden, L.A. & Estes, J.E. (1984) Bound-cation exchange affects the lag phase in actin polymerization. *Biochemistry* **23**, 2199–2203.
35. Combeau, C. & Carlier, M.-F. (1988) Probing the mechanism of ATP hydrolysis on F-actin using vanadate and the structural analogs of phosphate BeF_3 and AlF_4. *J. Biol. Chem.* **263**, 17429–17436.
36. Fisher, A.J., Smith, C.A., Thoden, J.B., Smith, R., Sutoh, K., Holden, H.M. & Rayment, I. (1995) X-ray structures of the myosin motor domain of *Dictyostelium discoideum* complexed with $MgADPBeF_x$ and $MgADPAlF_4$. *Biochemistry* **34**, 8960–8972.
37. Allen, P.G., Laham, L.E., Way, M. & Janmey, P.A. (1996) Binding of phosphate, aluminum fluoride, or beryllium fluoride to F-actin inhibits severing by gelsolin. *J. Biol. Chem.* **271**, 4665–4670.
38. Blake, R.D. (1987) Cooperative lengths of DNA during melting. *Biopolymers* **26**, 1063–1074.
39. Conejero-Lara, F., Mateo, P.L., Aviles, F.X. & Sanchez-Ruiz, J.M. (1991) Effect of Zn^{2+}on the thermal denaturation of carboxypeptidase B. *Biochemistry* **30**, 2067–2072.
40. Sanchez-Ruiz, J.M. (1992) Theoretical analysis of Lumry-Eyring models in differential scanning calorimetry. *Biophys. J.* **61**, 921–935.
41. Sanchez-Ruiz, J.M., Lopez-Lacomba, J.L., Cortijo, M. & Mateo, P.L. (1988) Differential scanning calorimetry of the irreversible thermal denaturation of thermolysin. *Biochemistry* **27**, 1648–1652.
42. Galisteo, M.L., Mateo, P.L. & Sanchez-Ruiz, J.M. (1991) Kinetic study on the irreversible thermal denaturation of yeast phosphoglycerate kinase. *Biochemistry* **30**, 2061–2066.
43. Lepock, J.R., Ritchie, K.P., Kolios, M.C., Rodahl, A.M., Heinz, K.A. & Kruuv, J. (1992) Influence of transition rates and scan rate on kinetic simulations of differential scanning calorimetry profiles of reversible and irreversible protein denaturation. *Biochemistry* **31**, 12706–12712.
44. Schmid, F.X. (1992) Kinetics of unfolding and refolding of single-domain proteins. In *Protein Folding* (Creighton, T., ed.), pp. 197–241. Freeman, New York.
45. McLaughlin, P.J., Gooch, J.T., Mannherz, H.G. & Weeds, A.G. (1993) Structure of gelsolin segment 1-actin complex and the mechanism of filament severing. *Nature* **364**, 685–692.
46. Schutt, C.E., Myslik, J.C., Rozycki, M.D., Goonesekere, N.C.W. & Lindberg, U. (1993) The structure of crystalline profilin-beta-actin. *Nature* **365**, 810–816.
47. Chik, J.K., Lindberg, U. & Schutt, C.E. (1996) The structure of an open state of beta-actin at 2.65 Å resolution. *J. Mol. Biol.* **263**, 607–623.
48. Aspenström, P., Schutt, C.E., Lindberg, U. & Karlsson, R. (1993) Mutations in beta-actin: influence on polymer formation and on interactions with myosin and profilin. *FEBS Lett.* 163–170.
49. Mossakowska, M., Moraczewska, J., Khaitlina, S. & Strzelecka-Golaszewska, H. (1993) Proteolytic removal of three C-terminal residues of actin alters the monomer–monomer interactions. *Biochem. J.* **289**, 897–902.
50. Strzelecka-Golaszewska, H., Moraczewska, J., Khaitlina, S.Y. & Mossakowska, M. (1993) Localization of the tightly bound divalent-cation-dependent and nucleotide-dependent conformation changes in G-actin using limited proteolytic digestion. *Eur. J. Biochem.* **211**, 731–742.
51. Strzelecka-Golaszewska, H., Mossakowska, M., Wozniak, A., Moraczewska, J. & Nakayama, H. (1995) Long-range conformational effects of proteolytic removal of the last three residues of actin. *Biochem. J.* **307**, 527–534.
52. Page, R., Lindberg, U. & Schutt, C.E. (1998) Domain motions in actin. *J. Mol. Biol.* **280**, 463–474.
53. Guzman-Casado, M., Parody-Morreale, A., Mateo, P.L. & Sanchez-Ruiz, J.M. (1990) Differential scanning calorimetry of lobster haemocyanin. *Eur. J. Biochem.* **188**, 181–185.
54. Lepock, J.R., Rodahl, A.M., Zhang, C., Heynen, M.L., Waters, B. & Cheng, K.-H. (1990) Thermal denaturation of the Ca^{2+}-ATPase of sarcoplasmic reticulum reveals two thermodynamically independent domains. *Biochemistry* **29**, 681–689.
55. Morin, P.E., Diggs, D. & Freire, E. (1990) Thermal stability of membrane-reconstituted yeast cytochrome *c* oxidase. *Biochemistry* **29**, 781–788.
56. Arriaga, P., Menendez, M., Villacorta, J.M. & Laynez, J. (1992) Differential scanning calorimetric study of the thermal unfolding of β-lactamase I from *Bacillus cereus*. *Biochemistry* **31**, 6603–6607.
57. Arroyo-Reyna, A. & Hernandez-Arana, A. (1995) The thermal denaturation of stem bromelain is consistent with an irreversible two-state model. *Biochim. Biophys. Acta* **1248**, 123–128.
58. Villaverde, J., Cladera, J., Padros, E., Rigaud, J.-L. & Dunach, M. (1997) Effect of nucleotides on the thermal stability and on the deuteration kinetics of the thermophilic F_0F_1 ATP synthase. *Eur. J. Biochem.* **244**, 441–448.
59. Villaverde, J., Cladera, J., Hartog, A., Berden, J., Padros, E. & Dunach, M. (1998) Nucleotide and Mg^{2+} dependency of the thermal denaturation of mitochondrial F1-ATPase. *Biophys. J.* **75**, 1980–1988.
60. Vogl, T., Jatzke, C., Hinz, H.-J., Benz, J. & Huber, R. (1997) Thermodynamic stability of annexin VE17G: equilibrium parameters from an irreversible unfolding reaction. *Biochemistry* **36**, 1657–1668.
61. Menendez, M., Rivas, G., Diaz, J.F. & Andreu, J.M. (1998) Control of the structural stability of the tubulin dimer by one high affinity bound magnesium ion at nucleotide N-site. *J. Biol. Chem.* **273**, 167–176.
62. Meijberg, W., Schuurman-Wolters, G.K., Boer, H., Scheek, R.M. & Robillard, G.T. (1998) The thermal stability and domain interactions of the mannitol permease of *Escherichia coli*. *J. Biol. Chem.* **273**, 20785–20784.
63. Shakhnovich, E.I. & Finkelstein, A.V. (1989) Theory of cooperative transitions in protein molecules I. Why denaturation of globular proteins is a first-order phase transition. *Biopolymers* **28**, 1667–1680.
64. Shrake, A. & Ross, P.D. (1992) Origins and consequences of ligand-induced multiphasic thermal protein denaturation. *Biopolymers* **32**, 925–940.
65. Wittinghofer, A. (1997) Aluminum fluoride for molecule of the year. *Curr. Biol.* **7**, R682–R685.
66. Waechter, F. & Engel, J. (1977) Association kinetics and binding constants of nucleoside triphosphates with G-actin. *Eur. J. Biochem.* **74**, 227–232.
67. Frieden, C. & Patane, K. (1988) Mechanism for nucleotide exchange in monomeric actin. *Biochemistry* **27**, 3812–3820.
68. Sheterline, P., Clayton, J. & Sparrow, J.C. (1998) Actin. *Protein Profile* **4**, 1–272.
69. Wriggers, W. & Schulten, K. (1997) Stability and dynamics of G-actin:

back-door water diffusion and behavior of a subdomain 3/4 loop. *Biophys. J.* **73**, 624–639.

70. Mockrin, S.C. & Korn, E.D. (1980) *Acanthamoeba* profilin interacts with G-actin to increase the rate of exchange of actin-bound adenosine 5′-triphosphate. *Biochemistry* **19**, 5359–5362.
71. Tobacman, L.S. & Korn, E.D. (1982) The regulation of actin polymerization and the inhibition of monomeric actin ATPase activity by *Acanthamoeba* profilin. *J. Biol. Chem.* **257**, 4166–4170.
72. Vinson, V.A., De La Cruz, E.M., Higgs, H.N. & Pollard, T.D. (1998) Interactions of *Acanthamoeba* profilin with actin and nucleotide bound to actin. *Biochemistry* **37**, 10871–10880.
73. DeVries, J.X., Schäfer, A.J., Faulstich, H. & Wieland, T. (1976) Protection of actin from heat denaturation by various phallotoxins. *Hoppe-Seylers Z. Physiol. Chem.* **357**, 1139–1143.
74. Moraczewska, J., Wawro, B., Seguro, K. & Strzelecka-Golaszewska, H. (1999) Divalent cation-, nucleotide-, and polymerization-dependent changes in the conformation of subdomain 2 of actin. *Biophys. J.* **77**, 373–385.
75. Kraulis, P.J. (1991) MOLSCRIPT: a program to produce both detailed and schematic plots of protein structures. *J. Appl. Cryst.* **24**, 946–950.